Published by :
http://www.ijert.org

International Journal of Engineering Research & Technology (IJERT)
ISSN: 2278-0181
Vol. 14 Issue 05, May-2025

Analysis of the Structural Performance of Hybrid Composite Beams Incorporating Checkered Steel Plates and Aramid Fibres

Shany Monachan
Mtech Student, Department of Civil Engineering MIT

Suji. P
Assistant Professor, Department of Civil Engineering MIT

ABSTRACT
The structural performance of aramid fiber composite beams and enclosed checkered steel plates is investigated in this work. Because of their enhanced mechanical qualities, composite beams made of many materials are being used in modern buildings on a larger scale. The concave and convex surface patterns of the checkered steel plate provide it with anti-skid qualities and resistance to bending. This is mixed with aramid fiber, which is known for its remarkable energy absorption capacity and high strength-to-weight ratio. The goal of the research is to evaluate the combined impacts of these materials on the overall structural behavior of the beams. To assess variables including load-bearing capacity, deflection characteristics, and failure mechanisms, the research makes use of both experimental testing and finite element analysis. It is expected that the results will aid in the creation of sophisticated composite materials for use in civil engineering, possibly resulting in improvements to cost-effectiveness, durability, and safety.

Keywords: **Aramid fibre, checkered steel plate, load bearing capacity, deflection**

1. INTRODUCTION

1.1. General Background

Structural beams are fundamental components in construction, serving as load-bearing elements that transfer loads from the structure's upper levels to its foundation. They play a crucial role in ensuring the stability, strength, and integrity of buildings and infrastructure. Beams are designed to withstand various types of loads, including dead loads (such as the weight of the structure itself), live loads (e.g., occupants, furniture), and environmental loads (e.g., wind, earthquakes). Different materials and configurations are used for beams based on the specific requirements of the structure and the anticipated loads.

Checkered steel plate encased beams are a new method in structural engineering that enhances the load-bearing capacity and structural integrity of beams in construction projects. This technique involves wrapping traditional beams with checkered steel plates, providing additional strength, durability, and resistance to various loads and environmental conditions. The use of checkered steel plates enhances load-carrying capacity and structural integrity, as the checkered pattern on the steel surface increases bonding area with concrete or other materials. The pattern also improves shear resistance, making the beam more resilient against lateral forces. These beams offer flexibility in design, allowing engineers to optimize beam dimensions, reinforcement configurations, and material choices to meet specific project requirements. The combination of steel and concrete in checkered steel plate encased beams results in a durable and long-lasting structural element, reducing maintenance requirements and ensuring the overall structure's longevity. In addition to their structural benefits, checkered steel plate encased beams can also contribute to the aesthetic appeal of a building or infrastructure project. They are widely used in commercial, industrial, and residential buildings, bridge engineering, and infrastructure projects like stadiums, airports, and high-rise buildings. In conclusion, checkered steel plate encased beams represent a valuable advancement in structural engineering, offering enhanced performance, versatility, and durability in various construction applications.

Aramid fiber, a versatile and high-performance material, has become a significant advancement in structural engineering. Its exceptional strength-to-weight ratio, durability, and resistance to environmental factors make it ideal for structural design and construction. Aramid fiber composite beams, such as Kevlar, have a high strength-to-weight ratio that surpasses steel's, making them strong yet lightweight. They are non-corrosive, making them suitable for harsh environmental conditions. These composite beams offer flexibility in design, allowing engineers to tailor beam configurations, shapes, and dimensions to specific project requirements. They also demonstrate exceptional fatigue and impact resistance, making them suitable for structures subjected to cyclic loading or

(This work is licensed under a Creative Commons Attribution 4.0 International License.)

International Journal of Engineering Research & Technology (IJERT)
ISSN: 2278-0181
Vol. 14 Issue 05, May-2025

sudden impact events. They also possess inherent electrical insulating properties and low thermal conductivity, making them suitable for applications requiring electrical insulation or thermal management. Aramid fiber composite beams are widely used in aerospace and defence applications, civil engineering, and automotive and sports equipment. They are used in aircraft components, rotor blades, ballistic protection systems, bridges, buildings, and infrastructure projects. In the automotive industry, they are used in vehicle components to reduce weight, improve fuel efficiency, and enhance crashworthiness. In conclusion, the introduction of aramid fiber as a composite beam represents a significant advancement in structural materials, offering unparalleled strength, durability, and versatility across various engineering disciplines.

1.2. Need of the Study

The study on numerical simulation and comparative analysis of checkered steel encased beams with aramid fiber serves several purposes in the field of structural engineering and construction. It explores innovative structural solutions by combining traditional materials like steel with advanced materials like aramid fiber composites, aiming to develop efficient and high-performance solutions for modern construction projects. The study evaluates the structural performance of checkered steel encased beams and aramid fiber composite beams, understanding their strengths, weaknesses, and capabilities under different loading conditions. This information is crucial for optimizing material usage, achieving cost-effectiveness, sustainability, and structural efficiency in building designs. The study also contributes to safety and reliability by assessing the load-carrying capacity, strength, and durability of checkered steel encased beams and aramid fiber composite beams. This assessment is vital for designing structures that can withstand various environmental and dynamic loads while maintaining structural integrity. The environmental impact of using checkered steel encased beams versus aramid fiber composite beams contributes to sustainable construction practices, as understanding their lifecycle costs, recyclability, and eco-friendliness helps make informed decisions. The study's findings on cost-effectiveness, maintenance requirements, and lifecycle costs of checkered steel encased beams and aramid fiber composite beams provide valuable insights for project planners, contractors, and stakeholders, leading to more efficient construction processes and optimized resource use. It also contributes to the advancement of the structural engineering and construction industry by introducing and evaluating innovative materials and design concepts.

2. LITERATURE REVIEW

2.1. General

This chapter presents the review of studies conducted on the history, performance and behaviour of checkered steel plate and aramid fibre and the properties of the above that affect the performance of the concrete beam. In addition, the studies related to numerical simulations also reviewed.

2.2. Checkered Steel Plate

Checker steel plates were used as reinforcement for concrete beams to increase ductility and flexural strength, with a focus on the roughness of the plates and their positioning. Experimental and numerical studies have been conducted on various types of steel-concrete composite beams, such as Steel Corrugated-Plate Coupling Beams (SCPCBs), High Strength U-shaped Steel-Encased Concrete Composite Beams (HUCBs), and Steel Plate-Reinforced Concrete Composite (SPRCC) beams. These studies focus on assessing the shear-carrying capacity, energy dissipation capability, flexural performance, and anti-explosion performance of such composite beams through a combination of experimental tests and finite element analysis (FEA). The results indicate that these composite beams exhibit high shear capacities, good ductility, excellent flexural performance, and good anti-explosion performance due to the unique configurations and materials used in their design. The experimental and numerical analyses provide valuable insights into the behavior and structural performance of checkered steel plate encased beams under various loading conditions.

Checkered steel plates are crucial for encasing beams in construction due to their mechanical behavior, bonding characteristics, corrosion resistance, and durability. These properties include tensile strength, modulus of elasticity, concrete bonding, adhesion properties, corrosion resistance, coating performance, galvanic corrosion potential, fatigue behavior, and environmental durability. Tensile strength is essential for withstanding tensile forces and preventing structural failure. The modulus of elasticity reflects the material's stiffness and deformation ability under load, influencing deflection and deformation characteristics. Bonding characteristics are assessed with concrete or other materials used in composite beam construction, ensuring effective load transfer and structural integrity. Adhesion properties are tested between checkered steel plates and coatings or coatings used for corrosion protection and surface enhancement. Corrosion resistance is assessed through coating performance, including exposure to harsh environmental conditions. Galvanic corrosion potential is also investigated when in contact with dissimilar metals or in aggressive environments. Finally, fatigue behavior is assessed to determine the ability of checkered steel plates to withstand cyclic loading and repetitive stress without fatigue failure.

Li- Lin Cao et al. (2021) The study presents a unique design for a U-shaped steel-encased concrete composite beam (HUCB) with improved flexural performance and high strength. In order to increase bending capacity, the

(This work is licensed under a Creative Commons Attribution 4.0 International License.)

International Journal of Engineering Research & Technology (IJERT)
ISSN: 2278-0181
Vol. 14 Issue 05, May-2025

HUCB design incorporates longitudinal steel reinforcements, circular rebar reinforcement, and shear studs joining concrete and U-shaped steel. Through theoretical computations, finite element analysis, and actual testing, the study seeks to understand the flexural behavior of the HUCB. The study also looks at how the flexural performance of the composite beam is affected by the concrete's compressive strength, the steel plate's yield strength, and the width of the concrete slab flange.

Alexander Tusnin (2022) Steel beams and a reinforced concrete slab make up steel-concrete constructions, which for optimal performance need consistent shear force transmission. To guarantee that the beam and the slab are connected, anchoring mechanisms are utilized. A steel-concrete beam with bent sections is part of the design; it is made up of galvanized steel beams that are partially buried in a concrete slab that is 90 mm thick. Shear forces are transmitted via the adhesion of concrete and galvanized steel without the need for anchoring mechanisms. Through experimental testing, galvanized steel plates implanted in concrete were shown to have shear resistance of between 0.248 and 0.415 MPa. Several computational tools for steel-reinforced concrete beams were used to test numerical models.

Jia-Qi (2022) The Steel Corrugated-Plate Coupling Beam (SCPCB), which has good lateral resistance and energy dissipation characteristics, is used as a coupling beam joining shear walls. Studies utilizing both experimental and computational methods were carried out to evaluate the SCPCBs' ability to carry shear loads and dissipate energy. Three specimens were tested as part of the research, with an emphasis on shear-cyclic and monotonic behaviours. Numerical simulations were performed using finite element analysis. The findings showed that, even with thin steel webs, SCPCBs had excellent shear capacities, strong ductility, and energy dissipation capabilities. In order to enhance the design, parameter studies were conducted, resulting in a lower restraining stiffness ratio for better SCPCB static and hysteretic behaviours.

Hala Metawei et al. (2019) The study looked at the flexural performance of beams reinforced with checker steel plates, both vertically and horizontally. It highlighted the advantages of roughening surfaces to improve ductility and bond as well as the use of checker steel plates. In order to improve the ductility and flexural strength of concrete beams, checker steel plates were employed as reinforcement; however, careful consideration was given to the placement and roughness of the plates. To examine the functionality and behavior of the beams, experimental experiments were carried out on concrete beams reinforced with checker steel plates that had varying levels of surface roughness.

Shiye Wang et al. (2019) In order to examine the bond strength and failure mechanism, the research ran trials on components made of checkered steel reinforced concrete (CSRC). For various embedded locations, the study developed a local bond strength-relative slip constitutive model and an average bond strength-loaded end slip constitutive model. The typical bond strength was found to be greatly enhanced by the checkered pattern, with the height of the pattern and transverse stirrup ratio having an impact.

Li- hua Chen et al. (2018) In order to examine failure processes, load-deflection curves, strain distribution, load-slipping curves, and slip distribution curves, the research performed static load tests on six simply-supported beams. In the investigation, the slip effect was taken into account while calculating deflection and slip strain at the interface in mid-span using an extra curvature approach. According to the trial findings, the innovative checkered steel-encased concrete composite beam design strengthened the link between the two materials, improving the mechanical qualities.

Mohamed Emara et al. (2018) With an emphasis on the application of demountable bolted connections, the study examines the behavior of steel I-beams placed in both regular and steel fiber-reinforced concrete. A novel formula is devised to evaluate the ultimate load depending on the interaction between the bolts and surface condition. The primary goal is to improve composite action by assessing the ultimate load of steel I-beams with short demountable fasteners and utilizing SFRC with better tensile strength. In order to simulate push-out specimens evaluated experimentally and validate the findings against experimental data, a finite element model numerical simulation was built.

Jixiang Dai et al. (2015) Concrete filled checkered steel tubes (CFCST) are novel composite constructions that improve the steel-to-concrete shear connection. Due to the critical role that the bond strength between steel and concrete plays in structural performance, research on bond-slip constitutive relationships has been conducted. Enhancing performance through high strength, stiffness, ductility, seismic resistance, and economic advantages has been the main goal of CFCST research. By using push-out tests on CFCST specimens to address the low average bond strength between steel tube and concrete, the study establishes a bond-slip constitutive model.

2.3. Aramid Fibre

Numerous composite constructions incorporating steel and aramid fiber composites have been the subject of comparative analysis and numerical simulations in diverse settings. Research has demonstrated that aramid fiber composites, including AFRP, greatly improve steel beams' structural performance. The application of aramid fibers in beam-column junctions has shown to decrease deflection, a sign of better structural performance under load. Furthermore, aramid laminates and steel plates used in composite targets have demonstrated improved anti-

(This work is licensed under a Creative Commons Attribution 4.0 International License.)

International Journal of Engineering Research & Technology (IJERT)
ISSN: 2278-0181
Vol. 14 Issue 05, May-2025

explosive properties, with certain configurations outperforming conventional steel plates in minimizing central deflection. These results demonstrate how aramid fiber composites may improve the overall performance, ductility, and strength of steel structures in a variety of applications.

Gargi Jaiswal et al. (2021) Hybrid fiberwebs were created by blending staple fibers of polypropylene and aramid, processing them into composites, and thoroughly testing them for mechanical performance. Following ASTM guidelines, the tensile characteristics of aramid and polypropylene fibers were assessed. An average of fifty values were obtained. For the purpose of assessing the compressive and shear properties of composite plates, specially made specimen fixtures were created. Extensive experimental setups were created employing cutting-edge methods including digital image correlation.

Elif Agcakoca & Esra Biyiklioglu (2020) The study's main goal is to determine how well steel beams reinforced with aramid fibre's function when subjected to impact loads. Impact loading is a type of dynamic load that can cause large deformations quickly, altering how structural parts behave. In order to increase the strength and decrease the displacement values of steel beams under impact, the research examines composite materials reinforced with aramid fiber-reinforced polymers (AFRP) through experimental testing. Both experimental and finite element investigations have demonstrated that the application of AFRP reinforcement in composite elements increases strength and decreases displacement values when compared to non-reinforced samples. The Soutis formula is used to characterize the laminate's undamaged nonlinear shear behavior, and a strain-based damage initiation and development law simulates shear damage.

Lei Yand et al. (2013) Bulletproof vests and armor systems are two examples of high-velocity impact applications that frequently employ aramid fiber composites. Because low-velocity impact damage might occur throughout the course of an aircraft structure's service life, the impact performance of aramid fiber composites is essential. Using both experimental and computational techniques, the study examines how low-velocity impacts the performance of aramid fiber-reinforced laminates. The study's intralaminar damage model is based on continuum damage mechanics, which includes the exponential damage development rule and Hashin failure criterion. The Soutis formula is used to characterize the laminate's undamaged nonlinear shear behavior, and a strain-based damage initiation and development law simulates shear damage.

Javier Malvar et al. (2004) Many scholars have put out numerical and mathematical models to describe the behavior of confined concrete. The study employed a concrete material model that was created for blast analysis and validated for triaxial stress routes. The test results on concrete cylinders and prisms contained by FRP composites conducted by Suter and Pinzelli, Karbhari and Gao, and Mirmiran and Shahawy were numerically evaluated. After developing a numerical model, test data was compared to the model, which demonstrated high agreement, for cylinders and prisms contained by aramid, carbon, and glass FRP wraps.

2.3. Summary

The study evaluated the structural performance of steel-concrete composite beams, including steel plate-reinforced concrete beams, steel beam-column connections, and steel corrugated-plate coupling beams. Numerical simulations were conducted to validate the behavior of the composite beams, using finite element models to predict connections and analyze shear capacities, ductility, and energy dissipation capabilities. The results showed good agreement between experimental and numerical analyses, emphasizing the structural efficiency and performance of the composite beams under different loading conditions.

AFRP composites enhance steel beams' load carrying capacity and stiffness, reducing local buckling and punching. They also improve steel beams' dynamic responses, reducing impact resistance and fire resistance. Adhesion between galvanized steel and concrete is crucial for efficient shear force transfer in steel-concrete structures. Aramid fiber wrapping decreases deflection in beam column joints,

improving strength and ductility during earthquakes. Innovative ASCT plates show improved anti-explosive effects, affecting stress wave propagation and failure modes.

3. METHODOLOGY

This section explains the properties of materials involved, work methodology and numerical simulation conducted at work.

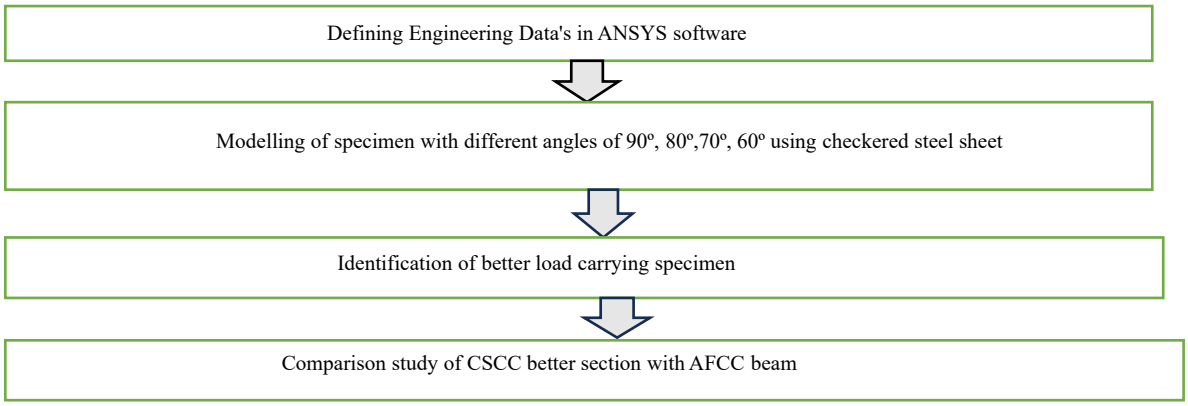

Fig.3.1. Methodology Flow Chart

(This work is licensed under a Creative Commons Attribution 4.0 International License.)

International Journal of Engineering Research & Technology (IJERT)
ISSN: 2278-0181
Vol. 14 Issue 05, May-2025

4. MATERIALS USED

4.1. Concrete (M25)

The material properties of M25 concrete, which is a commonly used grade of concrete in construction, include several key parameters that determine its strength, durability, and suitability for various structural applications.

Table 4.1. Properties of M25 Concrete

Mix	M25
Density	2400 kg/m³
Poisson's ratio	0.18
Young's modulus	25 GPa
Tensile strength	3.5 GPa

4.2. Checkered Steeel Plate

The material properties of checkered steel plates, also known as diamond plates or tread plates, are essential factors that determine their performance and suitability for various applications.

Table 4.2: Properties of checkered steel plate

Thickness	3 mm
Density	7850 kg/m³
Poisson's ratio	0.3
Young's modulus	250 MPa
Yield strength	250 MPa
Tensile strength	410 MPa

4.3. Aramid Fibre

Aramid fibers, such as those used in materials like Kevlar, possess unique material properties that make them highly desirable for a variety of applications, including structural reinforcement, protective gear, and aerospace components.

(This work is licensed under a Creative Commons Attribution 4.0 International License.)

International Journal of Engineering Research & Technology (IJERT)
ISSN: 2278-0181
Vol. 14 Issue 05, May-2025

Table 4.3: Properties of aramid fibre

Density (kg/m³)	1440
Moisture Absorption (%)	3.5
Yield Strength (Mpa)	3620
Elongation at Break (%)	2.4
Youngs Modulus (GPa)	112
Poisson's Ratio	0.28

5. NORMAL PCC BEAM

5.1. Modelling of a Normal PCC Beam

The dimension for a normal PCC beam will be Dimension = l×b×h = 1000mm×150mm×100mm
where, l= length, b=width, h=height
the support condition is fixed and Solid 65 is used for defining the concrete. The properties of concrete have been explained in table 4.1

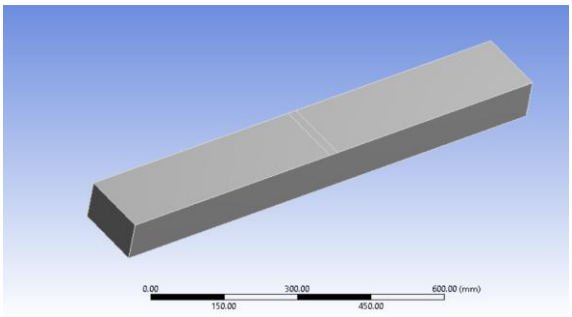

Fig:5.1. Modelling of a normal PCC beam

The model contains 132 elements and 931 nodes. The figure 5.2, 5.3, 5.4 shows the meshing, loading and deflection of normal PCC beam.

(This work is licensed under a Creative Commons Attribution 4.0 International License.)

International Journal of Engineering Research & Technology (IJERT)
ISSN: 2278-0181
Vol. 14 Issue 05, May-2025

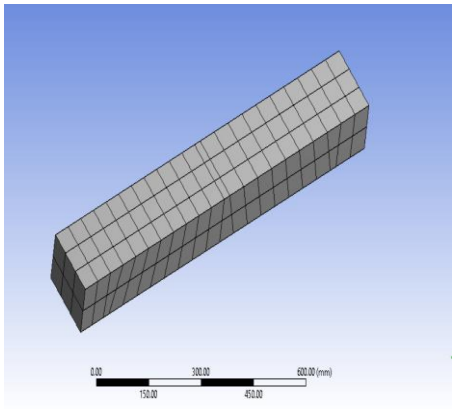

Fig: 5.2. Meshing of Normal PCC beam

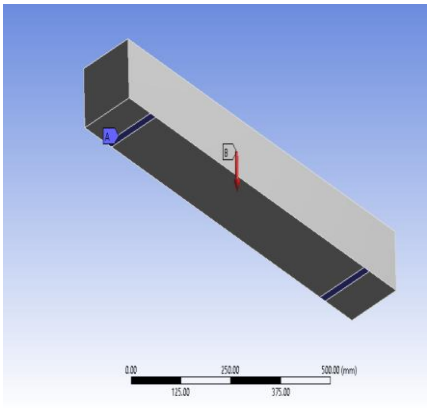

Fig:5.3. Loading of Normal PCC beam

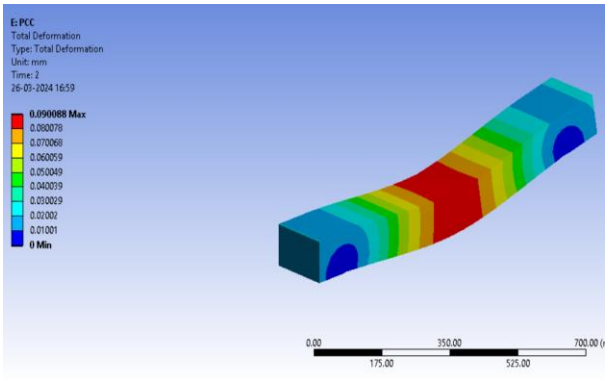

Fig:5.4. Deflection of Normal PCC beam

The load and deflection obtained is shown in table 5.1

Table 5.1. Load- Deflection values of PCC

Load(kN)	Deflection(mm)
6.25	0.09

The Load-Deflection graph is shown in figure 5.5

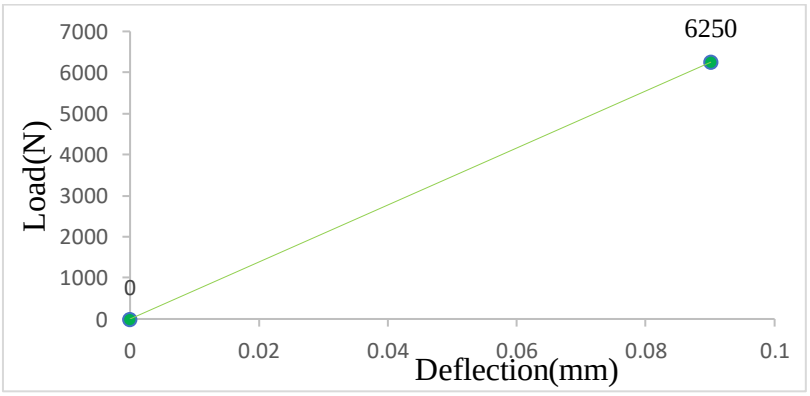

Figure 5.5 Load- Deflection Graph of PCC Beam

(This work is licensed under a Creative Commons Attribution 4.0 International License.)

Published by :
http://www.ijert.org

International Journal of Engineering Research & Technology (IJERT)
ISSN: 2278-0181
Vol. 14 Issue 05, May-2025

6. CHECKERED STEEL PLATE

6.1. Modelling of Checkered Steel Plate At 90º

The dimension for a normal PCC beam will be Dimension = l×b×h = 1000mm ×150mm×100mm

where, l= length, b=width, h=height

the support condition is fixed and Solid 65 is used for defining the concrete. The properties of concrete have been explained in table 4.2.

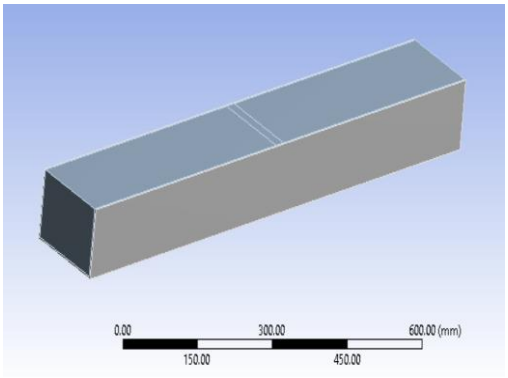

Fig 6.1. Modelling of checkered steel plate at 90º

The model contains 987 elements and 4760 nodes. The figure 6.2, 6.3, 6.4 shows the meshing, loading and deflection of checkered steel plate at 90 º.

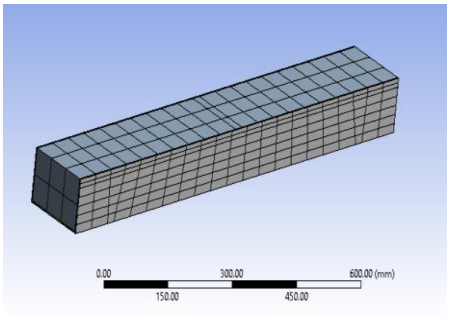

Fig 6.2. Meshing of CSP at 90º

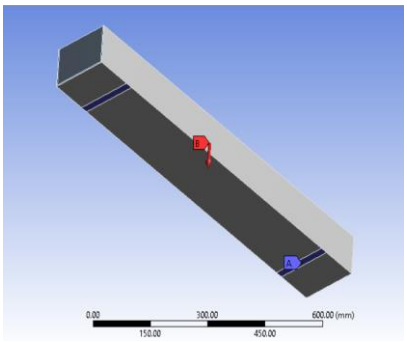

Fig 6.3. Loading of CSP at 90º

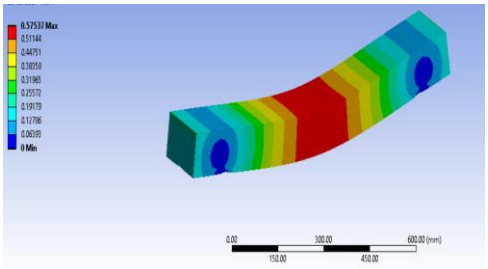

Fig 6.4. Deflection of CSP at 90º

The load and deflection values obtained are shown in table 6.1

Table 6.1 Load – deflection values of CSCC 90º

Load(kN)	Deflection(mm)
24	0.575

(This work is licensed under a Creative Commons Attribution 4.0 International License.)

International Journal of Engineering Research & Technology (IJERT)
ISSN: 2278-0181
Vol. 14 Issue 05, May-2025

The Load – Deflection graph is shown in figure 6.5

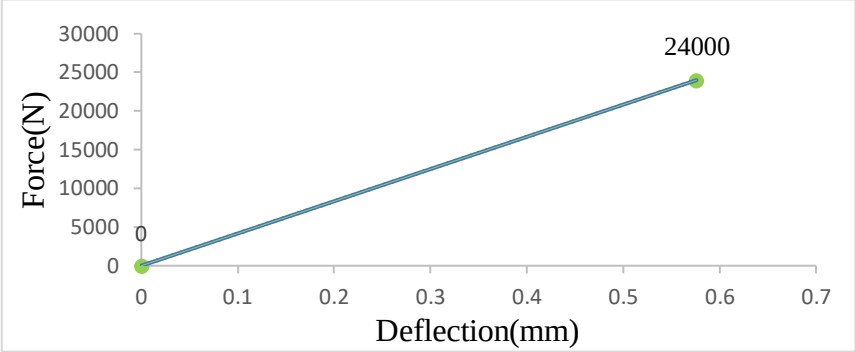

Fig 6.5. Load- Deflection graph of CSCC 90º

6.2. Modelling of Checkered Steel Plate At 80º

The dimension for a normal PCC beam will be Dimension = l×a×b×h =1000mm ×168mm×132mm ×100mm

where, l= length, b=width, h=height

the support condition is fixed and Solid 65 is used for defining the concrete. The properties of concrete have been explained in table 4.2.

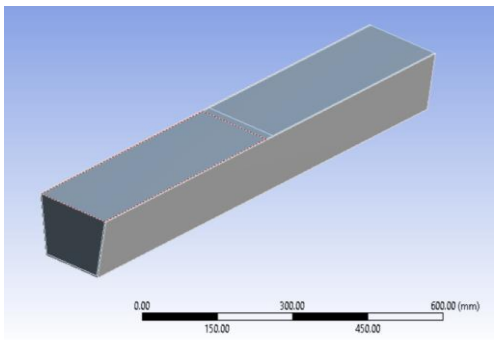

Fig 6.6. Modelling of checkered steel plate at 80º

The model contains 5606 elements and 12623 nodes. The figure 6.7, 6.8, 6.9,shows the meshing, loading and deflection of checkered steel plate at 80 º.

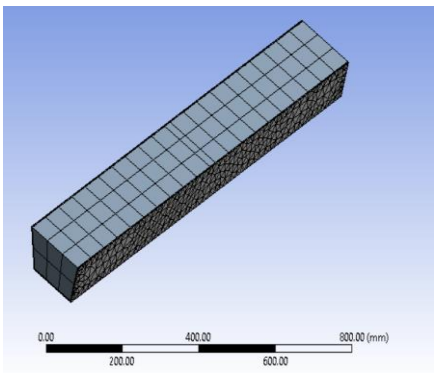

Fig 6.7. Meshing of CSP at 80º

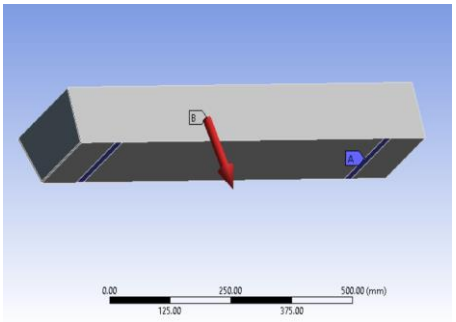

Fig 6.8. Loading CSP at 80º

(This work is licensed under a Creative Commons Attribution 4.0 International License.)

International Journal of Engineering Research & Technology (IJERT)
ISSN: 2278-0181
Vol. 14 Issue 05, May-2025

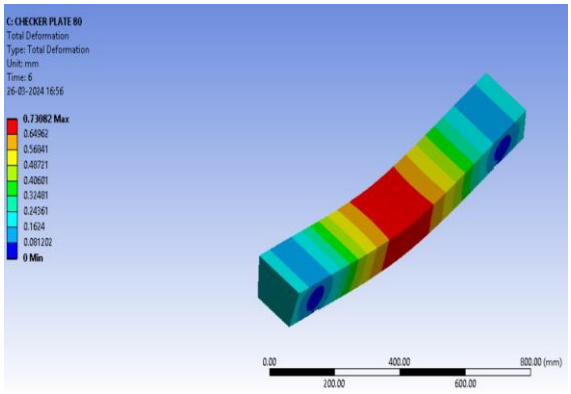

Fig 6.9. Deflection of CSP at 80º

The load and deflection obtained are shown in table 6.2

Table 6.2. Load – Deflection values of CSCC 80º

Load(kN)	Deflection(mm)
28	0.731

The load- deflection graph is shown in figure 6.10

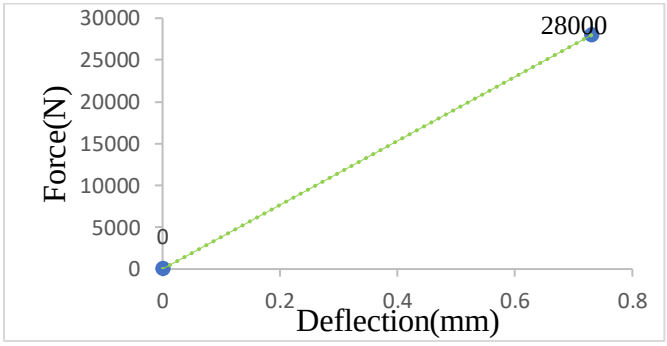

Fig 6.10. Load – Deflection graph

6.3. Checkered Steel Plate At 70º

The dimension for a normal PCC beam will be Dimension = l×a×b×h =1000mm ×186mm×114mm ×100mm
where, l= length, b=width, h=height
the support condition is fixed and Solid 65 is used for defining the concrete. The properties of concrete have been explained in table 4.2.

(This work is licensed under a Creative Commons Attribution 4.0 International License.)

Published by :
http://www.ijert.org

International Journal of Engineering Research & Technology (IJERT)
ISSN: 2278-0181
Vol. 14 Issue 05, May-2025

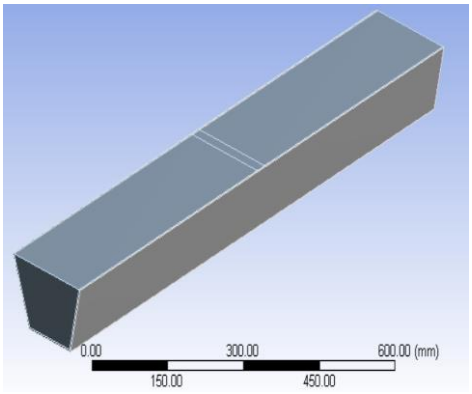

Fig 6.11. Modelling of Checkered steel plate at 70º

The model contains 630 elements and 4386 nodes. The figure 6.12, 6.13, 6.14 shows the meshing, loading and deflection of checkered steel plate at 70 º.

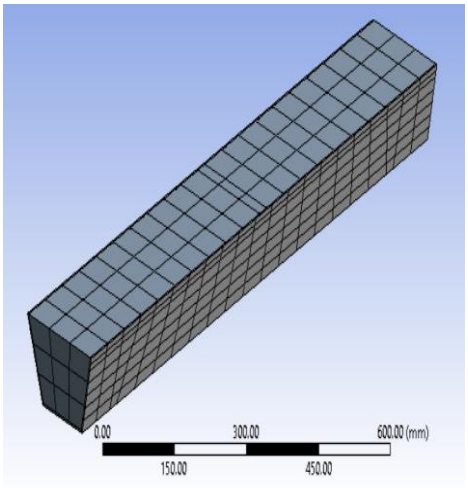

Fig 6.12. Meshing of CSP at 70º

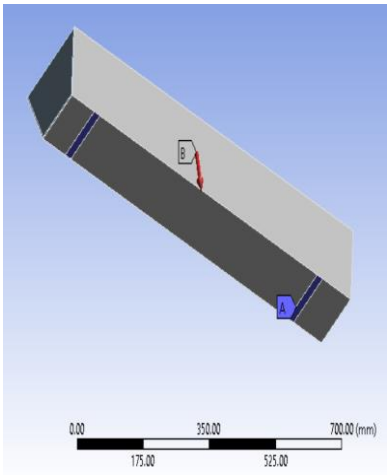

Fig 6.13. Loading of CSP at 70º

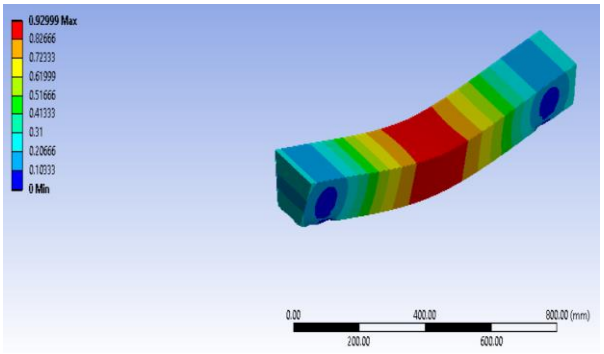

Fig 6.14. Deflection of CSP at 70º

The load and deflection values are shown in table 6.3

Table 6.3. Load – deflection values of CSCC 70°

Load(kN)	Deflection(mm)
34	0.930

(This work is licensed under a Creative Commons Attribution 4.0 International License.)

International Journal of Engineering Research & Technology (IJERT)
ISSN: 2278-0181
Vol. 14 Issue 05, May-2025

The load – deflection graph is shown in fig 6.15.

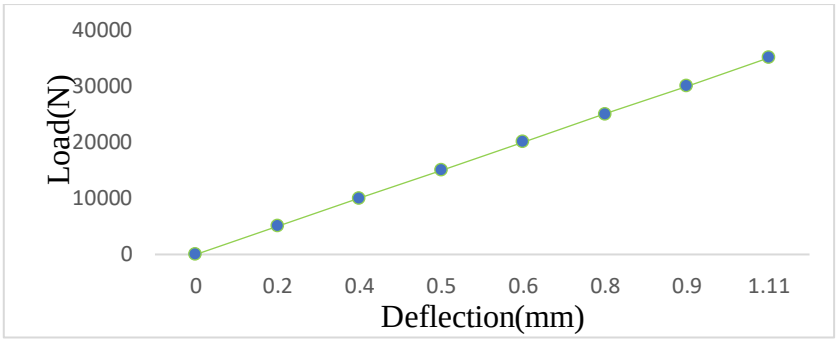

Fig 6.15. Load- deflection graph of CSCC 70°

6.4. Modelling of Checkered Steel Plate At 60º

The dimension for a normal PCC beam will be Dimension = l×a×b×h =1000mm ×208mm×92mm ×100mm

where, l= length, b=width, h=height

the support condition is fixed and Solid 65 is used for defining the concrete. The properties of concrete have been explained in table 4.2.

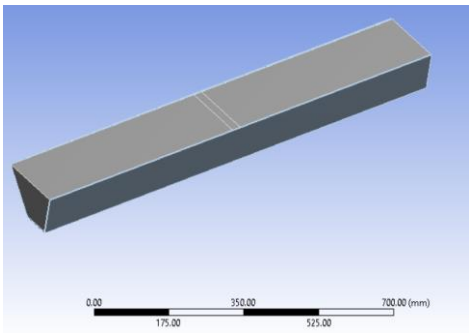

Fig 6.16. Modelling of checkered steel plate

The model contains 9535 elements and 52087 nodes. The figure 6.17, 6.18, 6.19 shows the meshing, loading and deflection of checkered steel plate at 60 º.

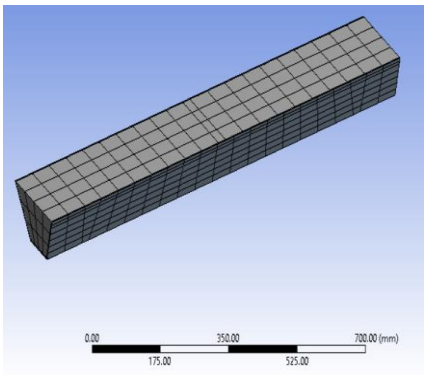

Fig 6.17. Meshing of CSP at 60º

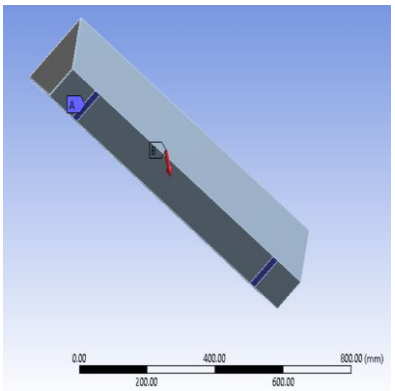

Fig 6.18. Loading of CSP at 60º

(This work is licensed under a Creative Commons Attribution 4.0 International License.)

International Journal of Engineering Research & Technology (IJERT)
ISSN: 2278-0181
Vol. 14 Issue 05, May-2025

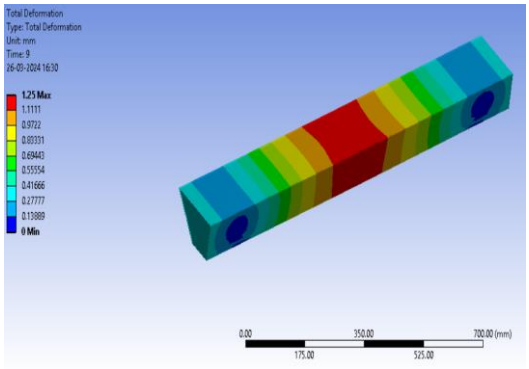

Fig 6.19. Deflection of CSPat 60º

The load and deflection values are shown in table 6.4

Table 6.4. Load- Deflection values of CSCC 60º

Load(kN)	Deflection(mm)
40	1.25

The load – deflection graph is shown in fig 6.20.

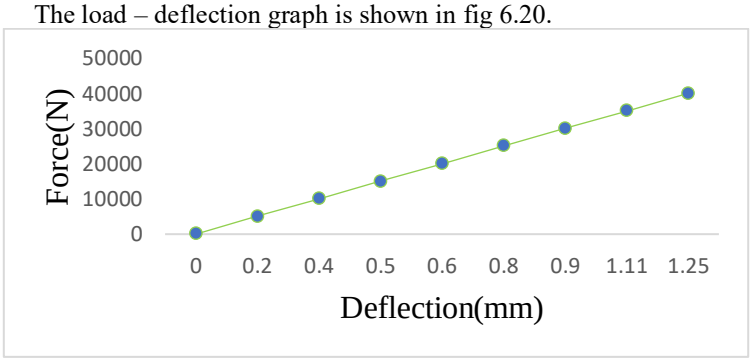

Fig 6.20. Load – Deflection Graph of CSCC 60º

7. ARAMID FIBRE

7.1. Modelling of Aramid Fibre At 60º

The dimension for a normal PCC beam will be Dimension = l×a×b×h =1000mm ×208mm×92mm ×100mm where, l= length, b=width, h=height

the support condition is fixed and Solid 65 is used for defining the concrete. The properties of concrete have been explained in table 4.3.

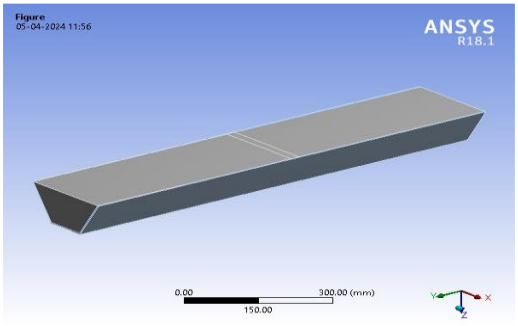

Fig 7.1. Modelling of Aramid Fibre at 60º

(This work is licensed under a Creative Commons Attribution 4.0 International License.)

International Journal of Engineering Research & Technology (IJERT)
ISSN: 2278-0181
Vol. 14 Issue 05, May-2025

The model contains 1008 elements and5562 nodes. The figure 7.2, 7.3, 7.4 shows the meshing, loading and deflection of Aramid fibre at 60 º.

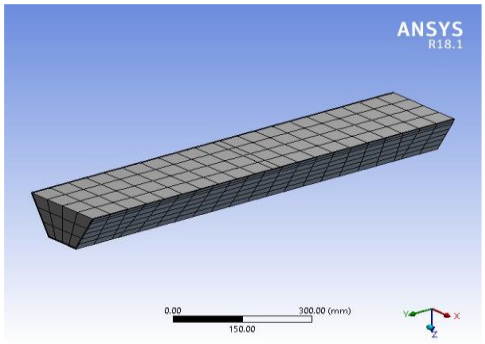

Fig 7.2. Meshing of AFCB at 60º

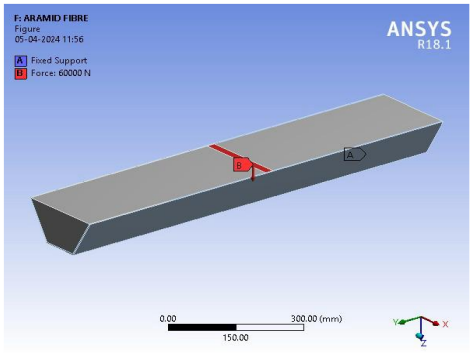

Fig 7.3. Loading of AFCB at 60º

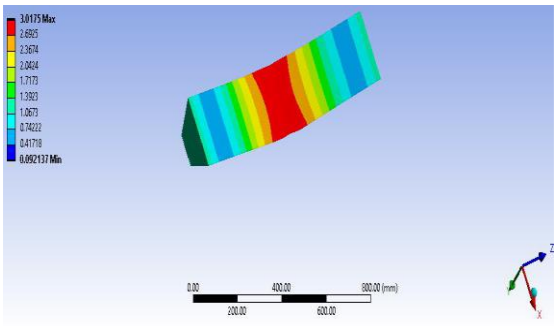

Fig 7.4. Deflection of Aramid fibre at 60º

The load and deflection values are shown in table 7.1.

Table 7.1. Load – Deflection values of Aramid fibre at 60º

Load (kN)	Deflection (mm)
60.738	3.01

The Load – deflection graph is shown in figure 7.5.

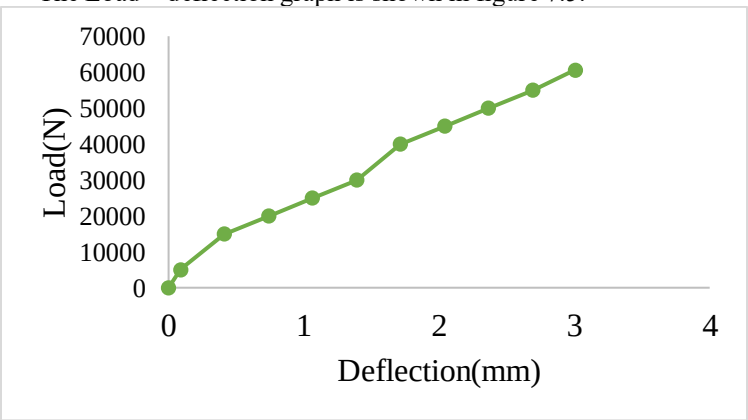

Fig 7.5. Load – deflection graph of Aramid fibre at 60º

(This work is licensed under a Creative Commons Attribution 4.0 International License.)

International Journal of Engineering Research & Technology (IJERT)
ISSN: 2278-0181
Vol. 14 Issue 05, May-2025

8. RESULTS AND DISCUSSION

Comparative bar diagram of the experimentally studied beams shown below.
The fluctuation in load according to the various cross-sectional angles is seen in figure 8.1 below.

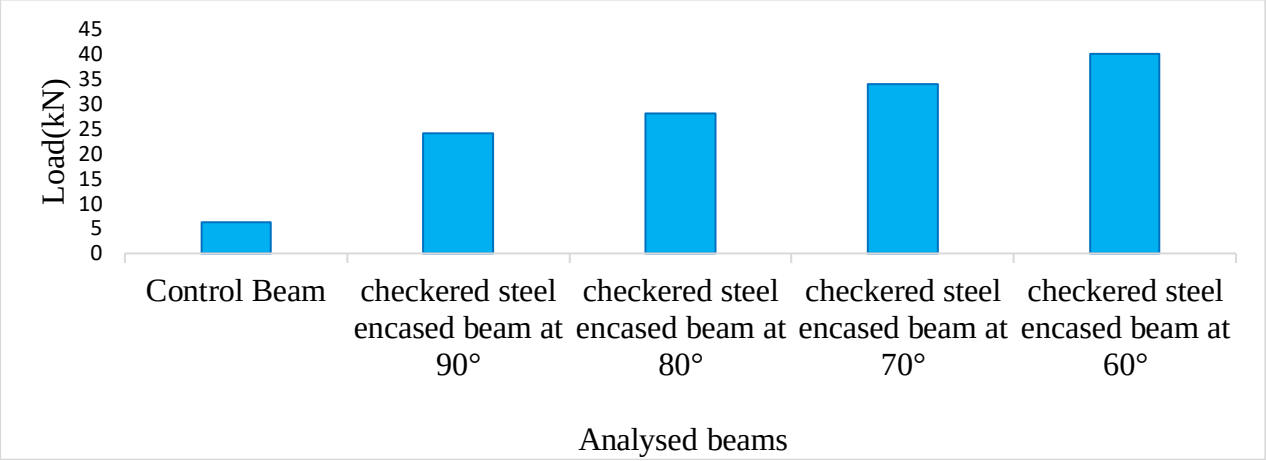

Fig 8.1. Comparative diagram of analysed beam

- In comparison to a plain cement concrete beam, which had an ultimate load of 6.25 kN and a deflection of 0.09 mm in the numerical study, the checkered steel encased beam carried a higher load of 24 kN with a 0.575 mm deflection.
- In comparison to other beams with angles of 90º, 80º, and 70º, the numerical results demonstrate that a checkered steel encased beam at 60º can support a load of 40kN with a deflection of 1.25 mm.
- The best part was determined to be the checkered steel encased beam at 60º.

The findings of a numerical analysis using ANSYS finite element software of a checkered steel encased beam at 60°, 70°, 80°, and 90° are displayed in table 8.1.

Table 8.1. Comparative study of PCC and Checkered steel plate

	PCC	Checkered steel plate at 90º	Checkered steel plate at 80º	Checkered steel plate at 70º	Checkered steel plate at 60º
Load	6.25	24	28	34	40
Deflection	0.09	0.575	0.731	0.930	1.25

Comparing the checkered steel-encased beam at 60° to the aramid fibre-encased beam at the same angle, the latter carried an ultimate load of 60.738 kN with a 3.01mm deflection.
Figure 8.2 displays the beams' comparison bar diagram.

(This work is licensed under a Creative Commons Attribution 4.0 International License.)

International Journal of Engineering Research & Technology (IJERT)
ISSN: 2278-0181
Vol. 14 Issue 05, May-2025

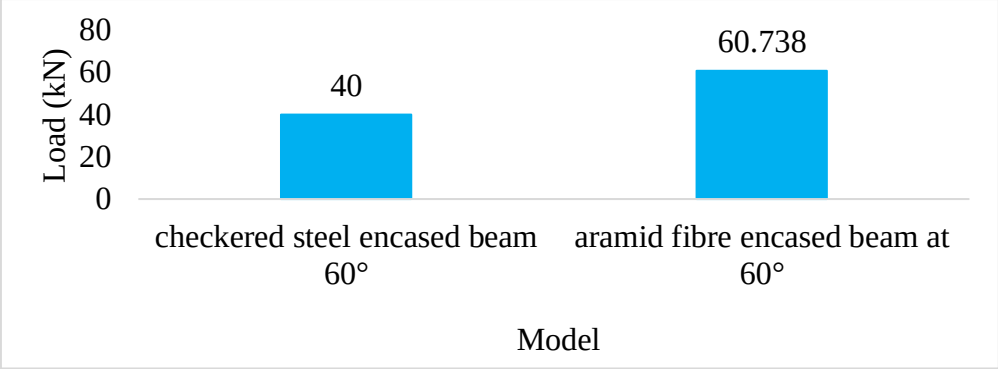

Fig 8.2. Comparative bar diagram of checkered steel plate and aramid fibre at 60°

9. CONCLUSION

With a particular focus on the performance of checkered steel encased beams and their appropriateness in structural applications, the numerical study carried out using ANSYS finite element software produced meaningful comparisons between various beam designs.

Considering the outcomes and talks that were given:

- Improved Load-Carrying Capacity: When compared to a plain cement concrete (PCC) beam, the checkered steel encased beam showed a noticeably higher ultimate load capacity. The PCC beam could only support loads up to 6.25 kN, however the checkered steel enclosed beam demonstrated its superior load carrying capacity with an ultimate load of 24 kN.
- Angle Optimization: Based on the numerical analysis, the checkered steel encased beam at a 60° angle showed the maximum load-carrying capability of 40 kN with a deflection of 1.25 mm among the several angles evaluated, which ranged from 90° to 60°. This result emphasizes how crucial angle adjustment is to improving these beams' structural performance.
- Comparative Analysis Using Beams Encased in Aramid Fibre: When a beam encased in aramid fiber was compared to a checkered steel beam at 60° at the same angle, the aramid fiber-encased beam had a greater ultimate load capacity, measuring 60.738 kN It's important to remember that there is a trade-off between load capacity and deflection behavior because the beam covered with aramid fiber also had a larger deflection of 3.01 mm.
- Ideal Configuration: The checkered steel encased beam at 60° is still a good option because of its balanced performance in load-carrying capacity and deflection, even if it has a somewhat lower load capacity than the aramid fiber-encased beam. The configuration that exhibited the highest level of performance out of all the parts examined was determined to be ideal for structural applications that need a blend of stiffness and strength.

The numerical research concludes that, when compared to conventional materials like plain cement concrete, checkered steel encased beams—especially when positioned at a 60° angle—are more successful in improving load-carrying capacity and structural performance. The results offer structural engineers and designers' useful information for maximizing beam designs for the best results in a range of engineering and building projects.

10. REFERENCES

1. Das, J., Butola, B. S., & Majumdar, A. (2025). Development of stab resistant Armor for different energy levels using shear thickening fluid reinforced multi-layered p-aramid fabrics. Polymer Composites, 46(2), 1843-1856.
2. Gao, Z., Wang, Z., Chen, Y., Li, S., Zhang, S., & Xu, L. (2024). Effect of structural configuration on the local explosion resistance performance of steel-aramid composite target plates. Engineering Fracture Mechanics, 307, 110302.
3. Hamoda, A., Elsamak, G., Emara, M., Ahmed, M., & Liang, Q. Q. (2023). Experimental and numerical studies of reinforced concrete beam-to-steel column composite joints subjected to torsional moment. Engineering Structures, 275, 115219. https://doi.org/10.1016/J.ENGSTRUCT.2022.115219
4. Dharmavarapu, P., & MBS, S. R. (2022). Aramid fibre as potential reinforcement for polymer matrix composites: a review. Emergent materials, 5(5), 1561-1578.
5. Pai, A., Kini, C. R., & Shenoy, S. (2022). Experimental and numerical studies of fiber metal laminates comprising ballistic fabrics subjected to shock impact. Composite Structures, 297, 115917.
6. Hingnekar, D. R., & Vyavahare, A. Y. (2022). Steel plate girders behaviour under shear loading. Materials Today: Proceedings, 65, 1186–1192. https://doi.org/10.1016/J.MATPR.2022.04.173

(This work is licensed under a Creative Commons Attribution 4.0 International License.)

International Journal of Engineering Research & Technology (IJERT)
ISSN: 2278-0181
Vol. 14 Issue 05, May-2025

7. Gargi Jaiswal a, Maloy K. Singha a, Dipayan Das (2021) Mechanical behavior of aramid-polypropylene fiberweb composites, Composite Structures 268 (2021) 113938
8. Dhanesh, S., Kumar, K. S., Maruthur, P., Rejumon, R., & Usmansha, G. S. (2021). Experimental investigation of strength of Aramid kelvar and chopped carbon reinforced concrete beam. Materials Today: Proceedings, 45, 1269–1273. https://doi.org/10.1016/J.MATPR.2020.04.730
9. Jaiswal, G., Singha, M. K., & Das, D. (2021). Mechanical behavior of aramid-polypropylene fiberweb composites. Composite Structures, 268, 113938. https://doi.org/10.1016/J.COMPSTRUCT.2021.113938
10. Zhang, X., Ding, Y., & Shi, Y. (2021). Numerical simulation of far-field blast loads arising from large TNT equivalent explosives. Journal of Loss Prevention in the Process Industries, 70, 104432.
11. Gholipour, G., Zhang, C., & Mousavi, A. A. (2020). Numerical analysis of axially loaded RC columns subjected to the combination of impact and blast loads. Engineering Structures, 219, 110924.
12. Durgesh R. Hingnekar, S.M. ASCE1; and Arvind Y. Vyavahare (2020) Mechanics of Shear Resistance in Steel Plate Girder: Critical Review American Society of Civil Engineers
13. Hingnekar, D. R., & Vyavahare, A. Y. (2020). Mechanics of Shear Resistance in Steel Plate Girder: Critical Review. Journal of Structural Engineering, 146(6), 03120001. https://doi.org/10.1061/(ASCE)ST.1943-541X.0002484
14. Ağcakoca, E., & Bıyıklıoğlu, E. (2020). Experimentally and numerically investigating the performances of aramid fiber-reinforced steel beams under impact loadings. Arabian Journal for Science and Engineering, 45(10), 8053-8068.
15. Hamoda, A., Emara, M., & Mansour, W. (2019). Behavior of steel I-beam embedded in normal and steel fiber reinforced concrete incorporating demountable bolted connectors. Composites Part B: Engineering, 174, 106996. https://doi.org/10.1016/J.COMPOSITESB.2019.106996
16. Chen, Lihua; Wang, Shiye; Yin, Chao; Li, Shutin (2019). Experimental study on constitutive relationship between checkered steel and concrete. Construction and Building Materials, 210(), 483–498. doi:10.1016/j.conbuildmat.2019.03.164.
17. Haijiang Zhang , Shanhua Xu , Biao Nie and Yaxin Wen (2019). Effect of corrosion on the fracture properties of steel plates. Construction and Building Materials 225 (2019) 1202 1213.
18. Chen, L., Li, S., Zhang, H., & Wu, X. (2018). Experimental study on mechanical performance of checkered steel-encased concrete composite beam. Journal of Constructional Steel Research, 143, 223–232. https://doi.org/10.1016/j.jcsr.2017.12.021
19. Rolfe, E., Kelly, M., Arora, H., Hooper, P. A., & Dear, J. P. (2018). Blast Performance and Damage Assessment of Composite Sandwich Structures. Blast Mitigation Strategies in Marine Composite and Sandwich Structures, 209-225.
20. Malvar, L. J., Morrill, K. B., & Crawford, J. E. (2004). Numerical Modeling of Concrete Confined by Fiber-Reinforced Composites. Journal of Composites for Construction, 8(4), 315–322. https://doi.org/10.1061/(ASCE)1090-0268(2004)8:4(315)

(This work is licensed under a Creative Commons Attribution 4.0 International License.)